PNAS
www.pnas.org

Supplementary Information for

Title: Intestinal commensal microbiota and cytokines regulate Fut2^{+} Paneth cells for gut defense

Author list:

Mariko Kamioka[1–4], Yoshiyuki Goto[2,5], Kiminori Nakamura[6], Yuki Yokoi[6], Rina Sugimoto[6], Shuya Ohira[6], Yosuke Kurashima[1–4,7], Shingo Umemoto[1,3,8], Shintaro Sato[1,9,10], Jun Kunisawa[2,4], Yu Takahashi[11], Steven E. Domino[12], Jean-Christophe Renauld[13], Susumu Nakae[14], Yoichiro Iwakura[15], Peter B. Ernst[3, 16-18], Tokiyoshi Ayabe[6] and Hiroshi Kiyono[1–3,18*]

1 Department of Mucosal Immunology, IMSUT Distinguished Professor Unit, The Institute of Medical Science, The University of Tokyo, Tokyo 108-8639, Japan.

2 International Research and Development Center for Mucosal Vaccines, The Institute of Medical Science, The University of Tokyo, Tokyo 108-8639, Japan.

3 Department of Medicine, School of Medicine and Chiba University-UCSD Center for Mucosal Immunology, Allergy and Vaccine (CU-UCSD cMAV), University of California San Diego, CA 92093, USA.

4 Laboratory of Vaccine Materials, Center for Vaccine and Adjuvant Research and Laboratory of Gut Environmental System, National Institutes of Biomedical Innovation, Health and Nutrition (NIBIOHN), Osaka 567-0085, Japan.

5 Division of Molecular Immunology, Medical Mycology Research Center, Chiba University, Chiba 260-8673, Japan.

6 Department of Cell Biological Science, Graduate School of Life Science, Faculty of Advanced Life Science, Hokkaido University, Hokkaido 001-0021, Japan.

7 Department of Innovative Medicine, Graduate School of Medicine, Chiba University, Chiba 260-8670, Japan.

8 Department of Otolaryngology & Head and Neck Surgery, Faculty of Medicine, Oita University, Oita 879-5593, Japan

9 Mucosal Vaccine Project, BIKEN Innovative Vaccine Research Alliance Laboratories, Research Institute for Microbial Diseases, Osaka University, Osaka 565-0871, Japan.

10 Department of Immunology and Genomics, Osaka City University Graduate School of Medicine, Osaka 545-8585, Japan.

11 Food Biochemistry Laboratory, Department of Applied Biological Chemistry, Graduate School of Agricultural and Life Sciences, The University of Tokyo, Tokyo 113-8657, Japan.

12 Department of Obstetrics and Gynecology, Cellular and Molecular Biology Program, University of Michigan Medical Center, Ann Arbor, MI 48109-5617, USA.

13 Ludwig Institute for Cancer Research and Université Catholique de Louvain, Brussels B-1200, Belgium.

14 Graduate School of Integrated Sciences for Life, Hiroshima University, Hiroshima 739-8528, Japan.

15 Center for Experimental Animal Models, Institute for Biomedical Sciences, Tokyo University of Science, Chiba 278-0022, Japan.

16 Division of Comparative Pathology and Medicine, Department of Pathology, University of California San Diego, CA, 92093, USA.

17 Center for Veterinary Sciences and Comparative Medicine, University of California, CA, 92093, USA.

18 Future Medicine Education and Research Organization, Department of Immunology, Graduate School of Medicine, Chiba University, Chiba 260-8670, Japan.

Corresponding author: Hiroshi Kiyono

Email: kiyono@ims.u-tokyo.ac.jp

This PDF file includes:

- Supplementary text
- Fig. S1 to S12
- Supplementary Table
- Movie legends for Supplemental Video 1, 2
- SI References

Materials and Methods

Immunohistochemistry

Small intestine was flushed several times with cold phosphate-buffered saline (PBS), fixed in 4% paraformaldehyde for 15 h at 4°C, and embedded in paraffin (Wako) or OCT compound (Sakura Finetek). Then, 5-μm-thick tissue sections were prepared by following standard protocols. For *in vitro* study, organoids were fixed in 4% paraformaldehyde for 30 min at room temperature and then incubated in 0.1% Triton X (Nacalai Tesque) and 5% goat serum in PBS to increase cell membrane permeability. Samples were then treated with purified anti-CD16/CD32 antibody (as Fc block; BD Pharmingen) and incubated with fluorescein isothiocyanate–labeled or tetramethylrhodamine B isothiocyanate–labeled *Ulex europaeus* agglutinin 1 (UEA-1) (Vector) to detect α(1,2)fucose. To detect Paneth cells, samples were incubated with unlabeled polyclonal rabbit anti-lysozyme antibody (DakoCytomation) for 15 h at 4°C. After washing with PBS, unlabeled anti-lysozyme antibody–treated samples were stained with Alexa Fluor 647–labeled anti-rabbit IgG (Jackson ImmunoResearch Laboratories, Inc.). To detect the plasma membrane, samples were incubated with mouse anti-E-cadherin antibody (BD Transduction Laboratories). After incubation and washing with PBS, samples were incubated with Alexa Fluor 594–labeled anti-mouse IgG (Thermo Fisher) as the secondary antibody. To detect α-defensin, samples were incubated with anti-α-defensin monoclonal antibody (clone 77-R63(1)). After incubation and washing with PBS, samples were incubated with Alexa Fluor 488–labeled anti-rat IgG (Jackson ImmunoResearch Laboratories, Inc.) as the secondary antibody. After counterstaining with 4′,6-diamidino-2-phenylindole (DAPI; Sigma-Aldrich), the specimens were examined under a confocal laser scanning microscope (LSM 800 with Airyscan, ZEISS; TCS SP2, Leica; or BZ-9000, Keyence).

Cell preparation and flow cytometry

Crypt region cells were isolated from small intestine as previously described(2). Isolated small intestines were opened longitudinally, washed with cold PBS, cut into 5-mm pieces, and then washed again three times with cold PBS. Tissue fragments were incubated in PBS containing 2 mM EDTA for 30 min on ice, vigorously shaken in cold PBS to remove villi, and suspended in cold PBS by using a 10-mL pipette. Tissue fragments were removed with a 70-μm cell strainer (Falcon). The supernatant, which was enriched for crypts, was passed through a 70-μm cell strainer to remove the remaining villi. Isolated crypts were pelleted by centrifugation at 200*g* for 5 min; suspended in fresh, cold PBS; and stained with (i) Pacific Blue–labeled anti-CD45 antibody (BioLegend) to identify and eliminate hematopoietic cells from analysis, (ii) allophycocyanin-labeled anti-CD24 antibody (BioLegend) to identify the Paneth cell–enriched population(3), and (iii) tetramethylrhodamine B isothiocyanate–labeled UEA-1 to detect α(1,2)fucose. Peridinin-chlorophyll-protein–labeled Via-Probe solution (BD Bioscience) was used to discriminate between dead and living cells.

Detection of *Fut2* expression by X-gal staining

Fut2 promoter activity in frozen sections of small intestine in *Fut2*$^{LacZ/+}$ mice was examined by using an X-gal staining kit (Invitrogen). When β-galactosidase is produced by the LacZ gene under the control of the *Fut2* promoter**,** X-gal **(**an analog of lactose) is hydrolyzed to produce a blue pigment. Therefore, cells with an active Fut2 promoter were identified as blue-colored cells(4).

Measurement of Paneth cell granule size

Tissue sections were prepared as described in **Immunohistochemistry** in the main manuscript. Paneth cell eosinophilic granules were stained with hematoxylin and eosin as described previously(5). For frozen sections, granules in Paneth cells (lysozyme$^+$ cells) were detected and their size was measured by using ImageJ software(6).

Analysis of purified Fut2$^+$ Paneth cells and Fut2$^-$ Paneth cells

For the analysis of purified Fut2$^+$ Paneth cells and Fut2$^-$ Paneth cells shown in Fig. 2d-f and Fig. S1, crypt cells were incubated with Zinpyr-1 (Santa Cruz Biotechnology) to detect Paneth cells and with DyLight 649–labeled UEA-1 (Vector) to detect α(1,2)fucose. A JSAN cell sorter was used for transcriptomics analysis and data collection, and the AppSan software was used for data analysis (Bay Bioscience). Fut2$^-$ Paneth cells (as Zinpyr-1$^+$ UEA-1$^-$ cells) and Fut2$^+$ Paneth cells (as Zinpyr-1$^+$ UEA-1$^+$ cells) were isolated from the ileum of Fut1-deficient mice (Fig. S1). Total RNA was isolated from Fut2$^-$ and Fut2$^+$ Paneth cells by using a PureLink RNA Micro Kit (Invitrogen), and DNA contamination was eliminated with PureLink DNase (Invitrogen). A complementary DNA (cDNA) library was prepared by using a SMART-Seq v4 Ultra Low Input RNA Kit for Sequencing (Clontech). Adapters were ligated onto both ends of the cDNA fragments. Both ends of the cDNA was sequenced using a NovaSeq 6000 Sequencing System (Illumina).

Preparation of mouse intestinal organoids and treatment with cytokines

Small-intestinal crypts were isolated from 8 to 12-week-old mice and the organoids were prepared as described previously(7). The organoids were cultured in Matrigel (BD Biosciences) and treated with mIL-22 (R&D Systems) (1, 10, and 100 ng/mL) for two days. The cultures were then washed with PBS and treated with cell recovery solution (BD Biosciences) for 30 min on ice. The recovered organoids were collected by centrifugation at 440*g* for 5 min.

Preparation of fecal samples

Fecal samples were prepared as previously described(8). Samples were air-dried overnight, powdered by using a bead beater–type homogenizer (Beads Crusher μT-12; TAITEC), and then dissolved in PBS for 1 h at 4°C. After centrifugation at 20,000*g* for 20 min, the supernatant was collected to measure α-defensin concentration.

Enzyme-linked immunosorbent assay

Sandwich enzyme-linked immunosorbent assay was performed as previously described(8). One-hundred-microliter aliquots of fecal samples or intestinal organoid culture medium were added to wells coated with 1 μg/mL α-defensin monoclonal antibody (clone 77R-5)(1) and incubated at 25°C for 2 h. After washing in PBS-Tween, 100 μL of 0.5 μg/mL biotinylated detection antibody (clone 77R-20)(1) was added at 25°C for 1 h. Then, the wells were incubated with 100 μL of streptavidin–horseradish peroxidase conjugate (GE Healthcare Biosciences) at 25°C for 1 h. After a final wash, 100 μL of 3,3′,5,5′-tetramethylbenzidine chromogen substrate buffer was added and the wells were incubated at 25°C for 30 min. The reaction was stopped by addition of 100 μL of 0.6 N H_2SO_4, and

absorbance values were determined at 450 nm by using a microplate reader (Multiskan FC, Thermo Fisher Scientific).

Visualization and quantification of Paneth cell granule secretion

Paneth cell granule secretion was visualized and quantified as previously described(9). Briefly, intestinal organoids were released from Matrigel by incubating the whole Matrigel in Cell Recovery Solution (Corning) on ice for 5 min. After washing with cold Advanced DMEM/F12, intestinal organoids were transferred to a collagen-coated 8-well chamber slide (Matsunami) at 100 intestinal organoids per well. Differential interference contrast images of Paneth cells before and 10 min after stimulation with 0.1 μM Carbamyl choline (CCh) were obtained by using a confocal microscope (A1, Nikon). Paneth cell granule secretion was quantified by measuring granule area using the NIS-Elements AR software (ver.5.11, Nikon).

Fecal microbiota transplantation

Fecal microbiota transplantation (FMT) was performed as reported previously(10). In short, mice were given ampicillin (1 g/L; Nacalai Tesque, Kyoto, Japan) in their drinking water for 7 days. One day before FMT, the ampicillin-containing water was replaced with sterile water. Fecal pellets were obtained from Fut2-deficient mice or IL-22–deficient mice or their littermate wild-type mice. After homogenizing one or two of the fecal pellets in 1 mL of water, the supernatants were orally administered to the ampicillin-treated mice. Feces were then collected from the recipient mice each week for five weeks after fecal transfer and the α-defensin concentration in the feces was determined by enzyme-linked immunosorbent assay.

Transmission electron microscopy analysis

Ileum was fixed at room temperature for 2 h in a solution containing 2.5% glutaraldehyde, 2% paraformaldehyde, and 0.05 M cacodylate buffer (pH 7.4). After being washed with cacodylate buffer three times on ice, the samples were fixed in 2% osmium tetroxide on ice for 2 h and dehydrated sequentially with 30%, 50%, 70%, and 90% ethanol for 5 min at each strength. Dehydrated samples were treated with propylene oxide twice for 5 min and then embedded in Epon812 resin mixture (TAAB Laboratories). Ultra-thin sections (70 nm) stained with 2% uranyl acetate and Reynolds lead solution were examined under a Hitachi H-7500 electron microscope.

Isolation of lamina propria cells

After removal of Peyer's patches, the duodenum and ileum were opened longitudinally and washed several times with ice-cold PBS. The duodenum and ileum were then cut into 1-cm pieces, which were incubated in 1 mM EDTA in PBS at 37 °C for 15 min with gentle shaking to remove epithelial cells, as previously described(11-13). The remaining tissues were finely minced and stirred for 30 min in RPMI-1640 Media (Thermo Fisher Scientific) containing 2% fetal calf serum and 0.5 mg/mL collagenase (Sigma-Aldrich); this process was repeated three times using fresh fetal calf serum and collagenase. The suspension was passed through a cell strainer (70-μm pore size) to remove undigested debris, the filtrate was centrifuged at 1,700 rpm for 5 min, and the resulting pellet of lamina propria cells was washed with RPMI-1640 containing 2% fetal calf serum. Finally, RNA was

isolated from the lamina propria cells and used for real-time reverse-transcription polymerase chain reaction analysis.

Isolation of RNA and real-time reverse-transcription polymerase chain reaction analysis

Total RNA from tissue and organoids was isolated with TRIzol reagent (Invitrogen) and cDNA was synthesized from the RNA by using a SuperScript VILO cDNA Synthesis Kit (Invitrogen). The specific primers (Hokkaido System Science, Co., Ltd) and universal probes (Roche) used for the real-time reverse-transcription polymerase chain reaction **(**RT-PCR) were as follows: *Fut2* (forward [F], 5′-gcggttcgtccattccta-3′; reverse [R], 5′-aaaggtacctgggcactcg-3′, probe No.76), *Lyz1* (F, 5′-ggcaaaaccccaagatctaa-3′; R, 5′-tctctcaccaccctctttgc-3′, probe No.46), *Rab1b* (F, 5′-gtcaggagcggttcagga-3′; R, 5′-tttcacgttggcgtaggact-3′, probe No.11), *Rab3d* (F, 5′-aagtgtgacctggaagacgaa-3′; R, 5′-gctggcctcaaagaactcaa-3′, probe No.62), *Rab8a* (F, 5′-tcaaagcaaaaatggacaaaaa-3′; R, 5′-tccactgtgatcttgactccat-3′, probe No.32), *Rab26* (F, 5′-tcctggctggtaccttcatc-3′; R, 5′-gccatccacatccagaactt-3′, probe No.105), *Rab27a* (F, 5′-cctgcagttatgggacacg-3′; R, 5′-ccctgaagaatgcagtggtt-3′, probe No.51), *Rab37* (F, 5′-ccaaccagtcctcttttgaca-3′; R, 5′-ccacgtctctctgggcatac-3′, probe No.100), *Gapdh* (F, 5′-tgtccgtcgtggatctgac-3′; R, 5′-cctgcttcaccaccttcttg-3′, probe No.80). RT-PCR analysis was performed with a LightCycler II Instrument (Roche Diagnostics) to measure gene expression levels. For *IL-17a*, a set of specific primers (F, 5′-tttaactcccttggcgcaaaa-3′; R, 5′-ctttccctccgcattgacac-3′), 2x SYBR Green qPCR Master Mix (Bimake), and a StepOne Real-Time PCR System (Thermo Fisher Scientific) were used.

Figures

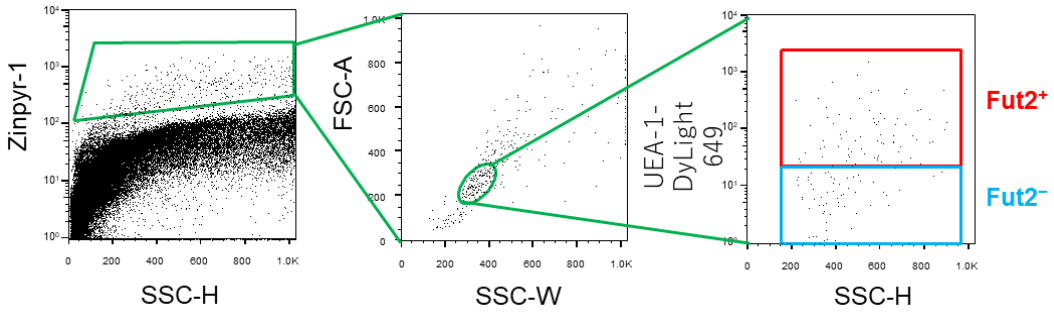

Fig. S1. Gating strategy for flow cytometric analysis and isolation of Fut2$^+$ and Fut2$^-$ Paneth cells

Zinpyr-1$^+$ cells were gated to obtain a highly purified fraction of Paneth cells, which was then gated using forward scatter area (FSC-A) and side scatter width (SSC-W) to obtain single Paneth cells. From the single Paneth cells, *Ulex europaeus* agglutinin-1–positive (UEA-1$^+$) cells were gated as Fut2$^+$ Paneth cells and UEA-1$^-$ cells were gated as Fut2$^-$ Paneth cells. SSC-H, side scatter height.

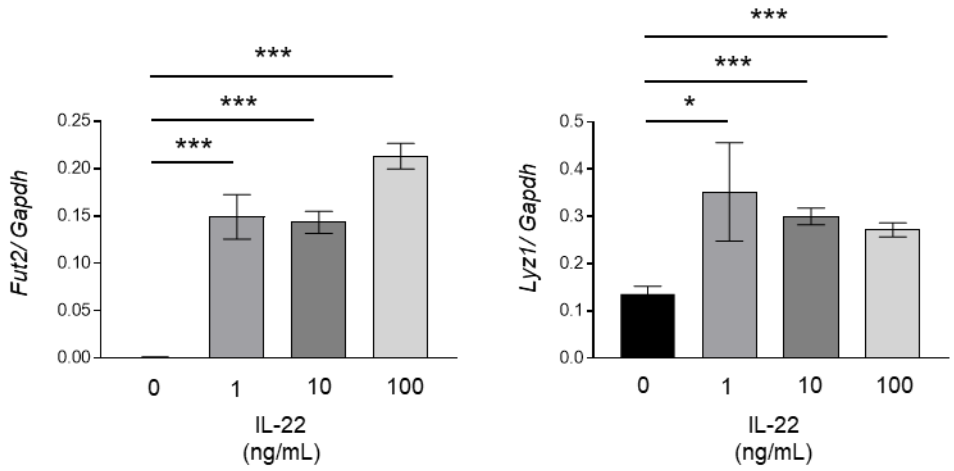

Fig. S2. Interleukin (IL) 22 induces upregulation of *Fut2* and *Lyz1* expression in organoids derived from duodenum of wild-type mice

Reverse-transcription polymerase chain reaction analysis of *Fut2* and *Lyz1* expression (relative to *Gapdh* expression) in organoids derived from duodenum of wild-type mice treated with the indicated concentrations of recombinant murine IL-22. Data are presented as mean ± SD (triplicate). **P* < 0.05, ****P* < 0.001, Student's *t*-test. Data are representative of two independent experiments.

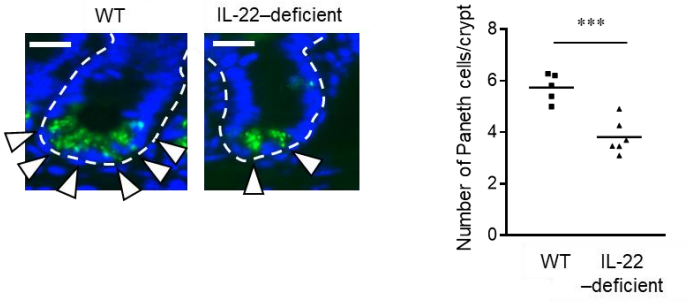

Fig. S3. Number of Paneth cells per crypt in ileum of wild-type (WT) and interleukin (IL) 22–deficient mice

Sections of ileum of WT and IL-22–deficient mice were stained with anti-lysozyme antibody (green) and DAPI (counterstain; blue) and the number of Paneth cells per crypt was counted. Left: White arrows indicate Paneth cells; white dotted lines delineate crypts. Bars: 20 μm. Right: Ten to fifteen crypts per mouse were examined. Five WT mice and six IL-22–deficient mice were analyzed. Horizontal lines indicate means. ***$P < 0.001$, Student's *t*-test.

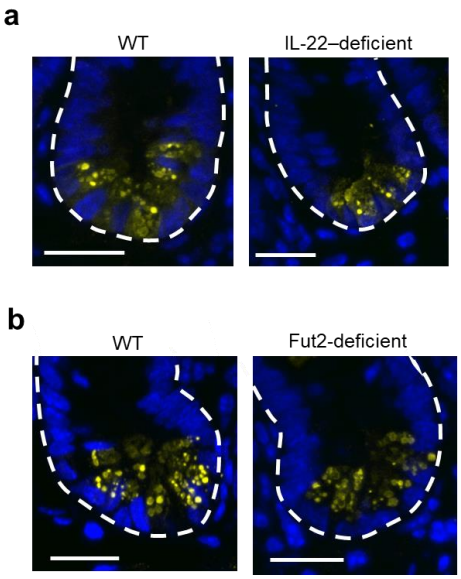

Fig. S4. Interleukin (IL) 22–deficient mice and Fut2-deficient mice express α-defensin in their Paneth cells

Sections of ileum from a) wild-type (WT) mice and IL-22–deficient mice and b) WT mice and Fut2-deficient mice were stained with anti-α-defensin (yellow) and DAPI (blue). White dotted lines delineate crypts. Bars: 20 μm. Images are representative of three independent experiments.

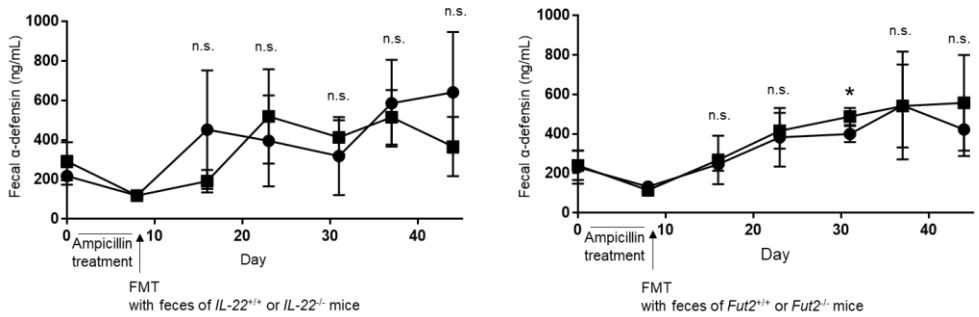

Fig. S5. α-Defensin concentration in the feces of mice after receiving fecal microbiota transplantation (FMT)

Mice were orally administered ampicillin for 7 days. On day 9, the mice were orally administered feces from interleukin 22 (IL-22)–deficient mice or Fut2-deficient mice or their littermate wild-type mice (*IL-22*$^{+/+}$ or *Fut2*$^{+/+}$). Feces were collected at week 1–5 after fecal transfer. α-Defensin concentration in the feces of FMT mice was measured by enzyme-linked immunosorbent assay. Circles, FMT mice that received with feces from WT mice. Squares, FMT mice that received feces from gene-deficient mice. Each group is $n = 5$. Error bars represent standard deviation of the mean. *$P < 0.05$, n.s., not significant, Student's *t*-test.

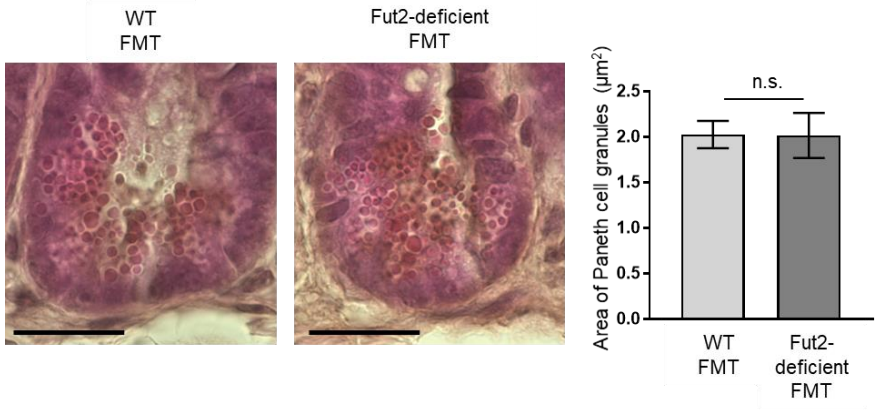

254

255 **Fig. S6. Size of Paneth cell granules in fecal microbiota transplantation (FMT) mice**

256 Mice were orally administered ampicillin for 7 days. On day 9, mice were orally administered feces
257 from wild-type (WT) or Fut2-deficient mice. On day 45, FMT mice were sacrificed and subjected to
258 hematoxylin and eosin staining to detect Paneth cell granules. Left: Bars = 20 μm. Right: Ten crypts
259 per mouse were examined, and Paneth cell granule area was measured with the ImageJ software(6).
260 Three mice per group were analyzed. Representative images are shown. Data are presented as
261 mean ± SD. n.s., not significant, Student's *t*-test.

262

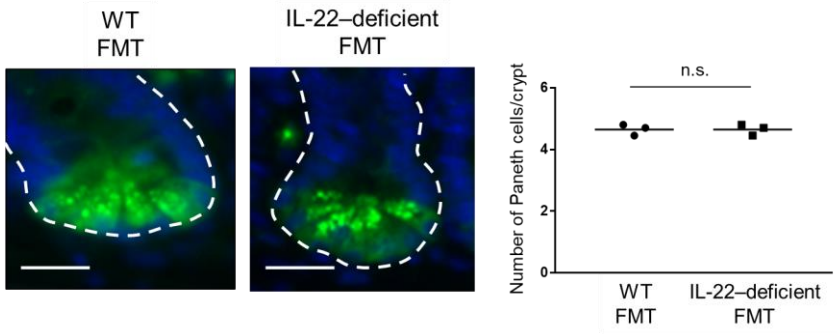

Fig. S7. Number of Paneth cells per crypt in ileum of fecal microbiota transplantation (FMT) mice

Mice were orally administered ampicillin for 7 days. On day 9, mice were orally administered feces from wild-type (WT) or IL-22–deficient mice. On day 45, FMT mice were sacrificed and subjected to immunohistological analysis to detect Paneth cells. Sections of ileum of FMT mice treated with feces from WT or IL-22–deficient mice were stained with anti-lysozyme antibody (green) and DAPI (counterstain; blue) and the number of Paneth cells per crypt was counted. Left: White arrows indicate Paneth cells; white dotted lines delineate crypts; bars = 20 μm. Right: Twenty crypts per mouse were examined. Three mice per group were analyzed. Horizontal lines indicate means. n.s., not significant, Student's *t*-test.

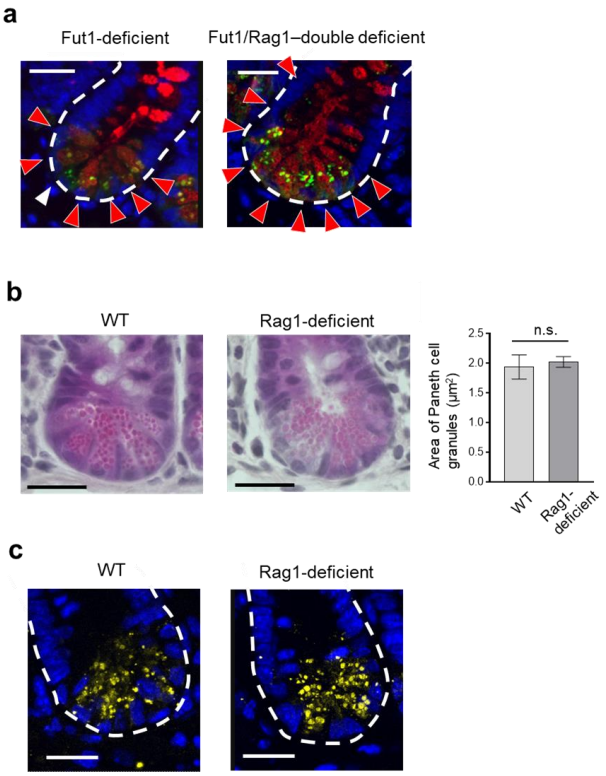

Fig. S8. Rag1-deficient mice possess Fut2⁺ Paneth cells and granules expressing α-defensin in their Paneth cells

a) Sections of ileum from Fut1-deficient mice and Fut1/Rag1–double deficient mice were stained with *Ulex europaeus* agglutinin-1 (UEA-1; red), anti-lysozyme antibody (green), and DAPI (counterstain; blue). Red arrows, lysozyme⁺ UEA-1⁺ cells; white arrow, lysozyme⁺ UEA-1⁻ cell; white dotted lines delineate crypts. Bars: 20 µm. Data are representative of three independent experiments.

b) Sections of ileum from wild-type (WT) (*n* = 3) and Rag1-deficient (*n* = 3) mice were subjected to hematoxylin and eosin staining to detect Paneth cell granules. Representative images are shown. Bars: 20 µm. Paneth cell granule area was measured in 10 crypts per mouse with the ImageJ software(6). Data are presented as mean ± SD. n.s., not significant, Student's *t*-test.

c) Sections of ileum from WT and Rag1-deficient mice were stained with anti-α-defensin (yellow) and DAPI (counterstain; blue). White dotted lines delineate crypts. Bars: 20 µm. Images are representative of three independent experiments.

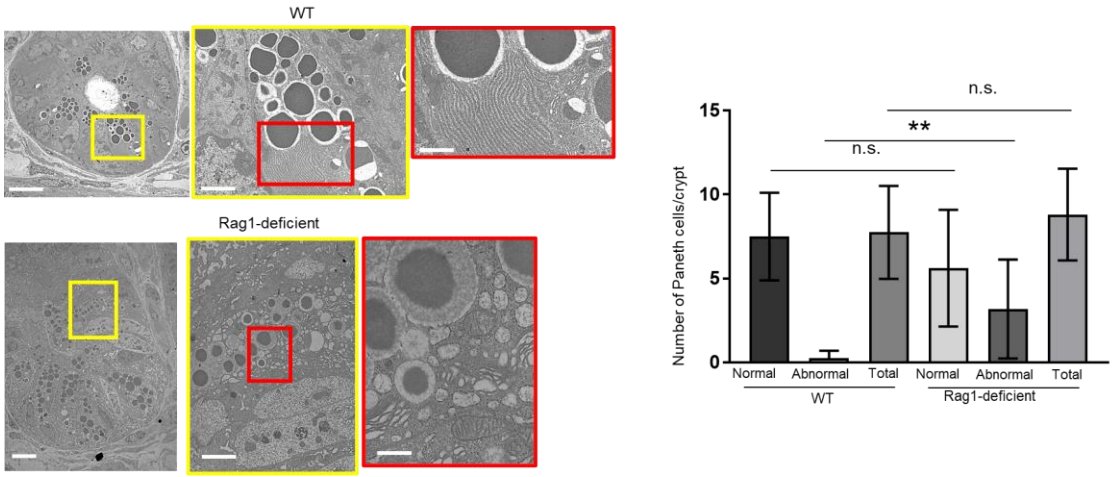

Fig. S9. Intracellular structure of crypt epithelial cells from wild-type (WT) and Rag1-deficient mice

Intracellular structure of crypt epithelial cells from WT and Rag1-deficient mice was analyzed by transmission electron microscopy. Bars: upper row: low magnification, 10 µm; medium magnification (yellow box), 2.5 µm; high magnification (red box), 1.3 µm; lower row: 10 µm, 2.9 µm, and 667 nm, respectively. Three to nine crypts from each type of mouse were observed per experiment. Images are representative of three independent experiments. Numbers of normal and abnormal Paneth cells per crypt were counted in 12 ileal crypts pooled from 3 WT mice, and 21 ileal crypts pooled from 3 Rag1-deficeint mice. Data are presented as mean ± SD. $^{**}P < 0.01$, Student's *t*-test. n.s., not significant.

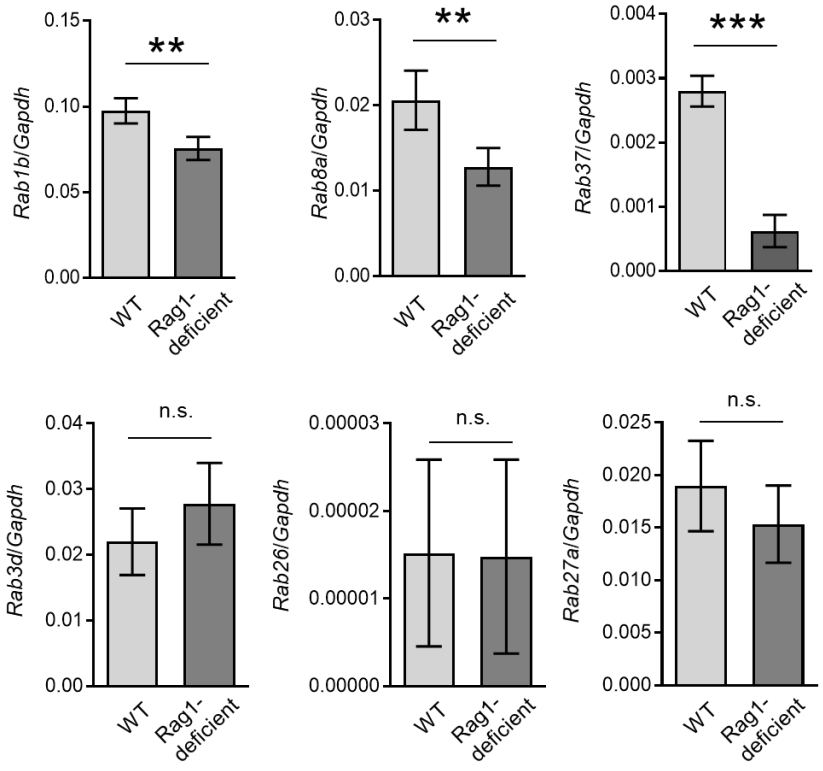

Fig. S10. Expression of Rab-family genes in ileal crypts of wild-type (WT) and Rag1-deficient mice

Reverse-transcription polymerase chain reaction analysis of *Rab1b*, *Rab8a*, *Rab37, Rab3d*, *Rab26*, and *Rab27a* expression (relative to *Gapdh* expression) in ileal crypts isolated from WT and Rag1-deficient mice. Data are presented as mean ± SD (WT mice, $n = 5$; Rag1-deficient mice, $n = 5$). $^{**}P < 0.01$ and $^{***}P < 0.001$, n.s., not significant, Student's *t*-test.

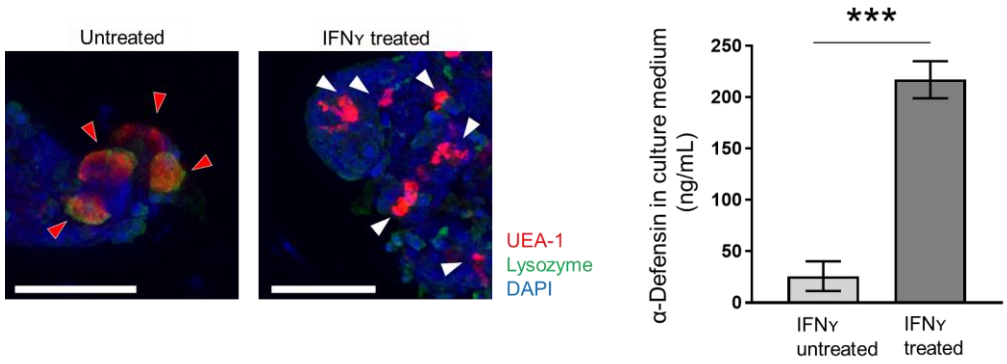

311

312 **Fig. S11. Interferon gamma (IFNγ) triggers degranulation of Paneth cells**

313 Organoids derived from duodenum of wild-type mice were treated with 5 ng/mL recombinant murine
314 IFNγ. Samples were stained with *Ulex europaeus* agglutinin-1 (UEA-1; red), anti-lysozyme antibody
315 (green), and DAPI (counterstain; blue). In a report by another group(14) UEA-1 was used to stain
316 Paneth cell granules. Red arrows indicate lysozyme$^+$ UEA-1$^+$ cells that possess granules; white
317 arrows indicate granule release into the crypt lumen. Bars: 50 μm. Data are representative of three
318 independent experiments. α-Defensin concentration in the intestinal organoid culture medium was
319 measured by enzyme-linked immunosorbent assay. Intestinal organoids derived from WT mice were
320 treated with 5 ng/mL recombinant IFNγ for 2 days. Four samples per group were analyzed. Data are
321 presented as mean ± SD; ***P < 0.001, Student's t-test.

322

323

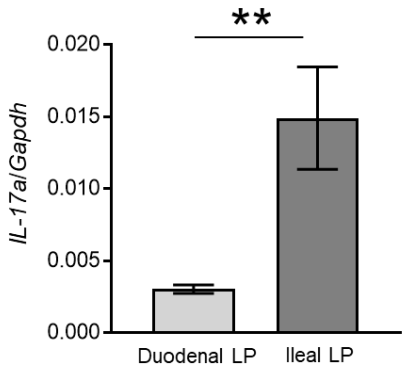

Fig. S12. Expression of *IL-17a* in duodenal and ileal lamina propria (LP) cells

Reverse-transcription polymerase chain reaction analysis of *IL-17a* expression (relative to *Gapdh* expression) in duodenal and ileal LP cells isolated from wild-type mice. Samples were obtained in triplicate per group. Data are presented as mean ± SD; $^{**}P < 0.01$, Student's *t*-test. Data are representative of three independent experiments.

Supplementary Table. Differentially Expressed Gene Analysis of Fut2^{+} Paneth Cells and Fut2^{-} Paneth Cells

Gene_ID	Transcript_ID	Gene_Symbol	Description	Fut2^{+}/Fut2^{-} Fold change
226413	NM_001081078	*Lct*	lactase	3.783418
216019	NM_145419	*Hkdc1*	hexokinase domain containing 1	2.063588
232714	NM_001171003	*Mgam*	maltase-glucoamylase	3.260019
69983	NM_001081137	*Sis*	sucrase isomaltase (alpha-glucosidase)	4.666254
209558	NM_134005	*Enpp3*	ectonucleotide pyrophosphatase/phosphodiesterase 3	3.601038
229927	NM_139148	*Clca3b*	chloride channel accessory 3B	2.115127
23844	NM_017474	*Clca1*	chloride channel accessory 1	3.965978
99709	NM_001033199	*Clca4b*	chloride channel accessory 4B	3.125216
16440	NM_080553	*Itpr3*	inositol 1,4,5-triphosphate receptor 3	2.231498
18797	NM_001290349,NM_008874	*Plcb3*	phospholipase C, beta 3	2.119382
11421	NM_001281819,NM_009598,NM_207624	*Ace*	angiotensin I converting enzyme (peptidyl-dipeptidase A) 1	2.065865
16535	NM_008434	*Kcnq1*	potassium voltage-gated channel, subfamily Q, member 1	2.085866
99663	NM_207208	*Clca4a*	chloride channel accessory 4A	2.721231
12638	NM_021050	*Cftr*	cystic fibrosis transmembrane conductance regulator	2.230965
13487	NM_021353	*Slc26a3*	solute carrier family 26, member 3	2.244970
27409	NM_031884	*Abcg5*	ATP-binding cassette, sub-family G (WHITE), member 5	2.043424
76408	NM_029600	*Abcc3*	ATP-binding cassette, sub-family C (CFTR/MRP), member 3	2.111202
20537	NM_019810	*Slc5a1*	solute carrier family 5 (sodium/glucose cotransporter), member 1	2.430809
105243	NM_001081060	*Slc9a3*	solute carrier family 9 (sodium/hydrogen exchanger), member 3	2.030977
18703	NM_011082	*Pigr*	polymeric immunoglobulin receptor	2.675044

Supplemental Video 1: Paneth cell granule secretion in untreated or Interleukin (IL) 22 treated organoids

Time-lapse images of Paneth cells in untreated or IL-22 treated organoids were taken by confocal microscopy after adding 0.1 μM carbamylcholine to the culture medium. Bars: 10 μm. Real acquisition time are represented by h:mm:ss (hour:minute:second).

Supplemental Video 2: Paneth cell granule secretion in organoids derived from wild-type (WT) and Fut2–deficient mice

Time-lapse images of Paneth cells in organoids derived from WT and Fut2–deficient mice were taken by confocal microscopy after adding 0.1 μM carbamylcholine to the culture medium. Bars: 10 μm. Real acquisition time are represented by h:mm:ss (hour:minute:second).

References

1 Eriguchi Y*, et al.* (2015) Decreased secretion of Paneth cell alpha-defensins in graft-versus-host disease. *Transpl Infect Dis* 17(5):702-706.

2. Sato T*, et al.* (2011) Paneth cells constitute the niche for Lgr5 stem cells in intestinal crypts. *Nature* 469(7330):415-418.

3. Wong VW*, et al.* (2012) Lrig1 controls intestinal stem-cell homeostasis by negative regulation of ErbB signalling. *Nat Cell Biol* 14(4):401-408.

4. Domino SE & Hurd EA (2004) LacZ expression in Fut2-LacZ reporter mice reveals estrogen-regulated endocervical glandular expression during estrous cycle, hormone replacement, and pregnancy. *Glycobiology* 14(2):169-175.

5. Rubio CA & Nesi G (2003) A simple method to demonstrate normal and metaplastic Paneth cells in tissue sections. *In Vivo* 17(1):67-71.

6. Schneider CA, Rasband WS, & Eliceiri KW (2012) NIH Image to ImageJ: 25 years of image analysis. *Nat Methods* 9(7):671-675.

7. Takahashi Y*, et al.* (2017) Reciprocal Inflammatory Signaling Between Intestinal Epithelial Cells and Adipocytes in the Absence of Immune Cells. *EBioMedicine* 23:34-45.

8. Nakamura K, Sakuragi N, & Ayabe T (2013) A monoclonal antibody-based sandwich enzyme-linked immunosorbent assay for detection of secreted alpha-defensin. *Anal Biochem* 443(2):124-131.

9. Yokoi Y*, et al.* (2019) Paneth cell granule dynamics on secretory responses to bacterial stimuli in enteroids. *Sci Rep* 9(1):2710.

10. Matsuo K*, et al.* (2019) Fecal microbiota transplantation prevents Candida albicans from colonizing the gastrointestinal tract. *Microbiol Immunol* 63(5):155-163.

11. Terahara K*, et al.* (2011) Distinct fucosylation of M cells and epithelial cells by Fut1 and Fut2, respectively, in response to intestinal environmental stress. *Biochem Biophys Res Commun* 404(3):822-828.

12. Goto Y*, et al.* (2014) Innate lymphoid cells regulate intestinal epithelial cell glycosylation. *Science* 345(6202):1254009.

13. Goto Y*, et al.* (2015) IL-10-producing CD4(+) T cells negatively regulate fucosylation of epithelial cells in the gut. *Sci Rep* 5:15918.

14. Farin HF*, et al.* (2014) Paneth cell extrusion and release of antimicrobial products is directly controlled by immune cell-derived IFN-gamma. *J Exp Med* 211(7):1393-1405.